

UV-Curable Contact Active Benzophenone Terminated Quaternary Ammonium Antimicrobials for Applications in Polymer Plastics and Related Devices

Lukas Porosa,[†] Alexander Caschera,[†] Joseph Bedard,[†] Amanda Mocella,[†] Evan Ronan,[†] Alan J. Lough,[‡] Gideon Wolfaardt,^{†,§} and Daniel A. Foucher^{*,†,§}

[†]Department of Chemistry and Biology, Ryerson University, 350 Victoria Street, Toronto, Ontario M5B 2K3, Canada

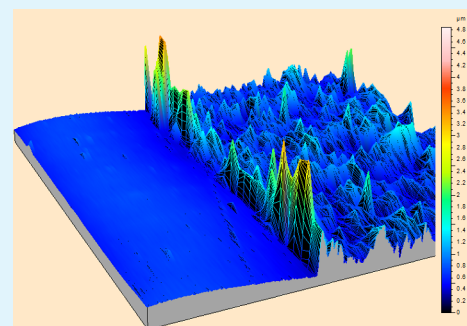
[‡]Department of Chemistry, University of Toronto, 80 St. George Street, Toronto, Ontario M5S 3H6, Canada

[§]Stellenbosch University Water Institute Secretariat, Faculty of Natural Science, Stellenbosch Central, Stellenbosch 7599, South Africa

S Supporting Information

ABSTRACT: A series of UV active benzophenone ($[\text{C}_6\text{H}_5\text{COC}_6\text{H}_4\text{-O}(\text{CH}_2)_n\text{-N}^+\text{Me}_2\text{R}][\text{X}^-]$; **4**, $\text{R} = \text{C}_{12}\text{H}_{25}$, $n = 3$, $\text{X}^- = \text{Br}^-$; **5a-c**, $\text{R} = \text{C}_{18}\text{H}_{37}$, $n = 3$, $\text{X}^- = \text{Cl}^-$, Br^- , I^- ; **6a-c**, $\text{R} = \text{C}_{18}\text{H}_{37}$, $n = 4$, $\text{X}^- = \text{Cl}^-$, Br^- , I^- ; **7a-c**, $\text{R} = \text{C}_{18}\text{H}_{37}$, $n = 6$, $\text{X}^- = \text{Cl}^-$, Br^- , I^-) terminated C_{12} and C_{18} quaternary ammonium salts (QACs) were prepared by thermal or microwave-driven Menshutkin protocols of the appropriate benzophenone alkyl halide (**1a-c**, **2a-c**, **3a-c**) with the corresponding dodecyl- or octadecyl *N,N*-dimethylamine. All new compounds were characterized by NMR spectroscopy, HRMS spectrometry, and, in one instance (**4**), by single-crystal X-ray crystallography. Representative C_{12} and C_{18} benzophenone QACs were formulated into 1% (w/v) water or water/ethanol-based aerosol spray coatings and then UV-cured onto plastic substrates (polypropylene, polyethylene, polystyrene, polyvinyl chloride, and polyether ether ketone) with exposure to low to moderate doses of UV ($20\text{--}30 \text{ J cm}^{-2}$). Confirmation as to the presence of the coatings was detected by advancing water contact angle measurements, which revealed a more hydrophilic surface after coating. Further confirmation was gained by X-ray photoelectron spectroscopy analysis, time of flight secondary ion mass spectrometry, and bromophenol blue staining, all of which showed the presence of the attached quaternary ammonium molecule. Analysis of surfaces treated with the C_{18} benzophenone **5b** by atomic force microscopy and surface profilometry revealed a coating thickness of $\sim 350 \text{ nm}$. The treated samples along with controls were then evaluated for their antimicrobial efficacy against Gram-positive (*Arthrobacter* sp., *Listeria monocytogenes*) and Gram-negative (*Pseudomonas aeruginosa*) bacteria at a solid/air interface using the large drop inoculum protocol; this technique gave no evidence for cell adhesion after a 3 h time frame. These antimicrobial materials show promise for their use as coatings on plastic biomedical devices with the aim of preventing biofilm formation and preventing the spread of hospital acquired infections.

KEYWORDS: environmentally friendly methods, Menshutkin, quaternary ammonium antimicrobials, UV cure, benzophenone coatings, plastics



1. INTRODUCTION

The global threat of infectious outbreaks and biofilm-related healthcare-acquired infections (HCAIs) caused by pathogenic microbial infestations has led to the adoption of aggressive, preventative approaches to combat the spread of such diseases. These approaches include improvement in cleaning protocols, spoiled laundry, and waste control, the widespread use of disinfectants, enforced hand washing procedures for healthcare staff, the ubiquitous use of disposable gloving, and new designs for hospital recovery rooms, Intensive Care Unit, and operating suites, all of which are designed to minimize the spread of pathogenic bacteria.¹ Despite these considerable efforts, the rate of infection remains unacceptable, and the numbers of postoperative deaths by infection is likewise still high. This situation creates a health and economic burden estimated at

billions of dollars per annum.² A major contributor to these infections and their related mortality rates is the presence of biofilms, which can support the cohabitation of pathogenic and nonpathogenic bacteria populations.³ Many of these biofilm producing microorganisms attach readily to porous and nonporous surfaces and proliferate in difficult to clean and sometimes unsuspected venues.⁴ Additionally, the over prescription of antibiotics to treat infectious diseases, as well as the extensive use of disinfectant chemicals and biocide-releasing antimicrobial surfaces, has led to the development of resistance by an ever-increasing number of strains of micro-

Received: May 24, 2017

Accepted: August 4, 2017

Published: August 4, 2017

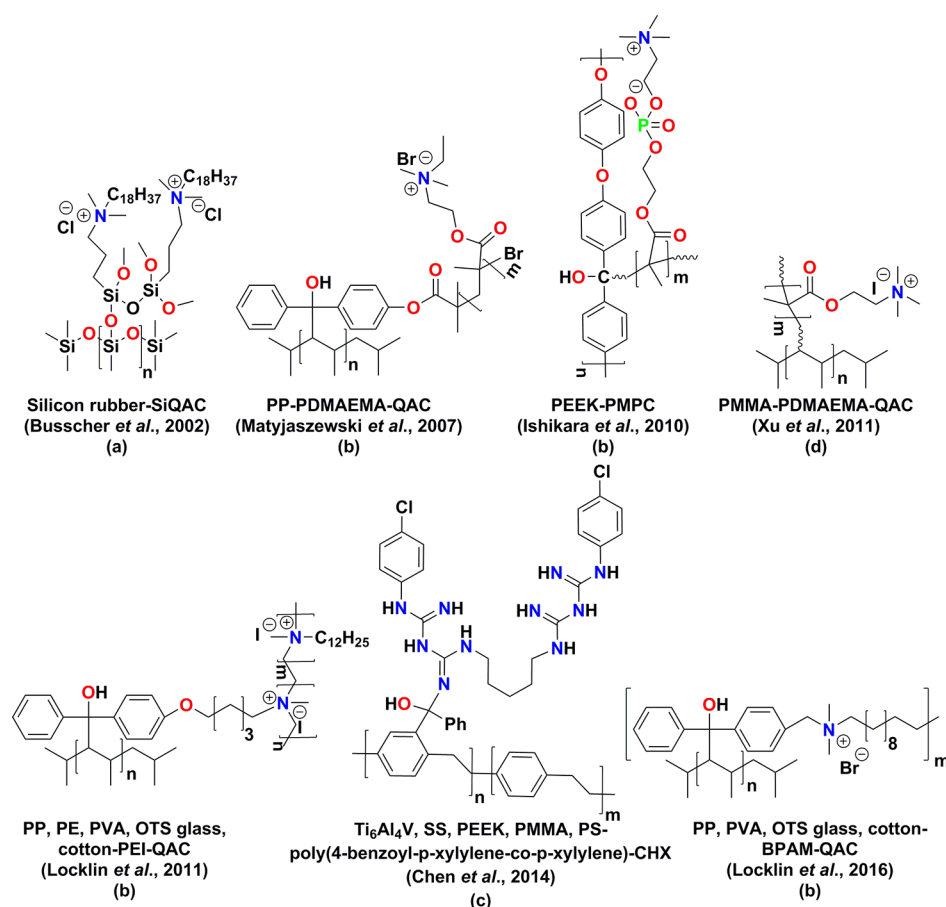


Figure 1. Examples from the literature of the covalent functionalization of plastic material surfaces with quaternary ammonium anchored biocides through (a) silane anchors, (b) benzophenone C–H insertions to surfaces or (c) grafting to a biocide, that is, chlorhexidine, CHX, or (d) acrylate photoinitiated by surface immobilized benzophenone.

organisms.⁵ When biofilms develop, microorganism survival is enhanced, and it is now understood that the majority of HCAIs (65–80%) are from pathogenic bacteria housed and released from such biofilms.⁶

In the mid-1960s, the Dow Corning Corp. developed a popular antibiofilm technology based on quaternary ammonium silanes (SiQAC, Figure 1); these materials can be readily grafted onto porous surfaces.⁷ These SiQAC were shown to be effective in preventing and combating biofilm formation by chemically altering surfaces with physically attached quaternary ammonium molecules. These areas include common touch points, air filters, sinks, hospital rooms, transport trucks, hospital uniforms, surgical equipment, medical devices, and everyday consumer products; all of these materials could be treated with covalently bonded quaternary ammonium antimicrobial nanoscale coatings.^{1,7–10} A clear advantage to the use of these surface-anchored bacteriostatic and bactericidal polycationic coatings (or “self-sterilizing antimicrobial surfaces”) is that they greatly reduce initial bacterial attachment by causing physical damage of microbial membranes upon physical contact. This is in contrast to conventional “leachable” biocides, which require cell uptake to disrupt the synthesis of proteins and/or weaken cell walls, or alternatively interfere with membrane function. All of these latter modes of action are susceptible to the development of drug resistance.^{11,12}

Modifying surfaces with immobilized, positively charged polymeric structures containing lipophilic moieties, such as long alkyl chains, has been shown to selectively interrupt the

function and integrity of microbial cell membranes with little or no effect on eukaryotic cells.^{9,12–14} Various “contact-killing” hypotheses have been proposed and are typically based on the proposed disruption of microbial membranes either by physical and/or electrostatic means or by their combination. The first contact killing hypothesis based on size was proposed in 2001 by Tiller *et al.* and is referred to as the “polymeric spacer” kill mechanism.¹⁵ Poly(vinylpyridine) (PVP) chains, of different molecular masses, were grafted onto amine-derivatized glass slides through a 1,4-dibromobutane cross-linker. This was followed by a second quaternization with alkyl bromides ranging in length from propyl to hexadecyl.¹⁵ Nonquaternized PVP slides displayed no antimicrobial effect as compared to unmodified control slides, while the highly quaternized poly(vinyl-*N*-hexylpyridinium) slides, specifically those grafted with shorter PVP chains (60 000 g mol⁻¹), showed <64% reduction of aerosol-deposited *Staphylococcus aureus* cells (24 h contact time with growth agar). Longer hexyl-PVP chains (160 000 g mol⁻¹) showed a 94% reduction of colony forming units (CFUs) over the same time period.^{15,16} A 4 log reduction (1 × 10⁶ CFU/mL) of *Escherichia coli* was achieved on amino-derivatized glass slides immobilized with sufficiently long (25 000–750 000 g mol⁻¹) *N*-hexyl or *N*-methyl-polyethylenimine (PEI) polymers. These materials had a surface charge density of 4.095 × 10¹⁵ [N⁺] cm⁻².¹⁷ Long, highly charged and flexible polycations grafted from polypropylene (PP) and microporous polypropylene membrane (MPPM) substrates also showed high antimicrobial activity. MPPM grafted at two

different charge densities (*E. coli* (2.11×10^{18} [N⁺] cm⁻²) and *S. aureus* (1.51×10^{18} [N⁺] cm⁻²)) with poly(2-(dimethylamino)ethyl methacrylate (PDMAEMA) by sequential UV-induced graft polymerization resulted in a 5.25 log reduction (1.75×10^5 CFU/mL) with 5 min contact time using the ASTM E2149 protocol (Figure 1).¹⁸ However, regardless of charge density and contact time, once the immobilized PDMAEMA lost its flexibility through cross-linking with *p*-xylylene dichloride, the antimicrobial activity was essentially zero.¹⁹ Complete (5.46 log, 2.88×10^5 CFU/mL) reductions in *E. coli* were obtained with PP slides (1 cm²) grafted with relatively high molecular weight (MW) PDMAEMA polymers (>9800 g mol⁻¹, $>1.40 \times 10^{15}$ [N⁺] nm⁻²) produced via atom transfer radical polymerization (ATRP). In contrast, low biocidal activity (<1 log) was observed for the surface grafted with shorter PDMAEMA chains (1500 g mol⁻¹, 2.00×10^{14} [N⁺] nm⁻²) after shaking (1 h with a 2.9×10^5 CFU/mL *E. coli* bacterial load) using the ASTM E2149 protocol.²⁰ To penetrate cell walls (16–80 nm thickness), surface grafted cationic polymers need to be long, flexible hydrophobic cations able to deliver an optimal balance of charge and hydrophobicity. Moderate hydrophobicity was achieved with either quaternized hexyl-PVP or hexyl PEI grafted polymers at constant positive charge. This enables the polymers to “stretch out” and avoid hydrophobic interchain aggregation.^{16,21}

A second contact killing hypothesis, one that is dominated by charge, is entitled the “phospholipid sponge”^{22,23} or “anion sponge”^{13,24} mechanism, which was proposed independently by Tiller et al. and Chen-Park et al. in 2011. This mechanism theorizes the removal of water-insoluble, negatively charged phospholipids and lipopolysaccharide (LPS) molecules from bacterial cell membranes upon close proximity and adequate contact time, with cationic antimicrobial surfaces lacking a long polymeric spacer. Once desorbed, negatively charged phospholipids of ~4.0 nm in length travel as liposomes through larger holes in the microbial cell wall to reach the attached cationic antimicrobial surface. Alternatively, such molecules become suctioned into the swollen pores (16.5 nm) of a polycationic hydrogel coating, resulting in membrane damage.¹³ A species-dependent, positive charge density, threshold on an amino-derivatized glass slide immobilized with poly(4-vinyl-*N*-butylpyridinium) bromide supports the charge-based mechanism with a 6.69 log reduction of both *Staphylococcus epidermidis* and *E. coli* with 1×10^{16} [N⁺] cm⁻² positive charge density. These results were noted after a 10 min contact time. When charge density values dropped below the threshold (5.6×10^{15} [N⁺] cm⁻²), a longer contact time (2 h) was needed to achieve complete kill of *S. epidermidis*.²⁵ With ATRP grafted PDMAEMA cationic polymer brushes, a 8×10^{15} [N⁺] cm⁻² charge requirement was needed to kill a monolayer of *E. coli* cells distributed over a 1 cm² surface area regardless of brush size (8 or 55 nm).²⁶ Cavallaro et al. used live dead staining with the nonpolymeric, surface immobilized glycidyltrimethylammonium chloride (GTAC) on plasma-polymerized amine-rich surfaces to evaluate efficacy. Using GTAC, a threshold of surface coverage concentration density of 4.2% quaternary bonded nitrogen sites with a minimum surface charge of +120.4 mV was required to reduce viable *E. coli* cells by 70.7% (2.5×10^6 CFU/mL).⁹ This suggests that the actual contact killing mechanism is a two-step process that is both charge and hydrophobicity driven.^{10,22} Bacteria are drawn in by localized powerful electrostatic adhesive forces (4–100 nN) or a simulated electric field when they approach a high charge

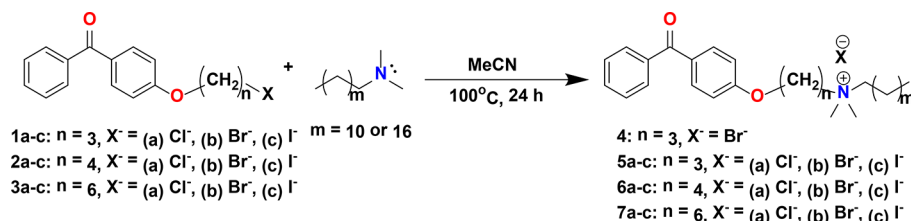
density cationic surface. These factors locally flatten out the membrane and establish a close proximity contact. Above the charge density threshold, bacteria are unable to detach and grow. This causes localized membrane damage with short architectures consisting of short hydrophobic residues via the phospholipid sponge mechanism. Larger features (consisting of long polymeric spacers: >30 nm) are able to insert and pierce the membrane through the polymeric spacer mechanism.¹⁴ Interestingly, 200 nm long irregularly shaped neutral surfaces, based on dragonfly wing nanopili, are able to cause localized microbial membrane damage in the absence of a positive charge.²⁷

Commodity-based plastic products have been well integrated into various industries, specifically, the medical and food industries where plastic serves as an essential material for medical devices and packaging. Unfortunately, plastic surfaces remain prone to biofilm formation.²⁸ Gottenbos et al. were the first to report an antibiofilm and antimicrobial plastic surface. This consisted of an oxidized –OH terminated silicone rubber, which was covalently modified with a SiQAC polymeric coating (Figure 1). A disadvantage of these materials is that the (inert) C–H terminated surface required argon plasma activation prior to grafting the antimicrobial.²⁹ Plasma activation requires expensive and complicated equipment, which can also damage or etch the polymer surface. In addition, the technique requires long grafting and curing periods with the SiQAC at high temperatures (20 h, 80 °C), conditions that are unsuitable for some plastic surfaces. Many studies have shown that when exposed to UV light, benzophenone type II photoinitiators form a diradical, which acts as a cross-linker for “grafting onto” plastic surfaces through a C–H insertion mechanism.³⁰ The diradical benzophenone group abstracts a hydrogen atom from neighboring aliphatic C–H groups at the polymeric surface, generating both surface radicals (R•) and semipinacol radicals (BP–OH•), which combine to form a C–C bond to the surface in the absence of monomer solutions.³¹ Alternatively, in the presence of acrylate monomers, the photoinduced radicals R• initiate surface grafted radical polymerization, which has been exploited to graft polymer brushes from common plastic surfaces. This can be done in either an uncontrolled or a controlled fashion by first immobilizing the photoinitiator to the surface.^{32,33}

A benzophenone-silane unit, first synthesized by Prucker et al., was designed as a bifunctional photo-cross-linker. This compound was successfully used to covalently bond SiO₂ surfaces to various C–H terminated polymer thin films through the benzophenone end group. Polystyrene (PS),³⁴ fluoropolymers,³⁵ hydrophilic polymers,³⁶ lipopolymers,³⁷ cholera toxin B subunit,³⁸ as well poly(oxanorbornene)-based synthetic mimics of antimicrobial peptides (SMAMPs)³⁹ have been used in the preparation of polyzwitterion/SMAMPs to act as antimicrobial surfaces.³⁹ Metal oxide surfaces of Al and Ti were similarly photochemically functionalized with poly(methyl methacrylate) (PMMA),⁴⁰ polyvinyl-*N*-methylacetamide (PNVA), poly(hydroxyethyl methacrylate) (PHEMA), and PS,⁴¹ respectively, through phosphonic acid benzophenone chemistries.

Benzophenone-substituted quaternary ammonium compounds (BPQACs) were first prepared in 1988 by Saetonne et al., for use in sunscreen formulations with limited antimicrobial properties,⁴² and later found uses as water-soluble photoaffinity tags for the photochemical immobilization of various biomolecules in biochemical research.^{43–45} They can

Scheme 1



also be used as water-soluble photoinitiators for photochemical hardening of acrylic monomers in ink, paint, and dye applications.^{46,47} Although the preparation of cationic contact-killing surfaces through either noncovalent or covalent means is well established in the literature, the application of BPQACs for the covalent modification of plastic surfaces for the attachment of cationic polymers is rather scarce with only a few reports describing their preparation. Matyjaszewski et al. were the first to report covalently attached polymer brushes through a commercially unpractical multistep “grafting from”, approach on PP through ATRP.⁴⁸ The benzophenone group in benzophenonyl 2-bromoisobutyrate was used as an anchor to promote the immobilization of ATRP initiator on PP from which PDMAEMA was grown and later quaternized with ethyl bromide.²⁰ When the PDMAEMA antimicrobial modified PP surfaces were tested using the ASTM E2149 protocol, a complete kill of *E. coli* (2.9×10^5 CFU/mL) was observed. The modified PP surface exhibited contact angles $>66^\circ$ with relatively high MW PDMAEMA ($M_n > 10\,000$ g mol⁻¹).²⁰

Locklin et al. reported covalent “grafting to” of cationic PEI polymer through benzophenone anchors onto various (C–H) terminated surfaces of commodity polymers (PP, PVC) as well as glass and cotton.^{49,50} Qualitative antimicrobial data, obtained via the spray inoculation method, were also detailed. Around the same time, we disclosed the syntheses of benzophenone-functionalized QACs comprising of a C₁₈ carbon chain coated on different plastic substrates. These materials were tested with the quantitative benchmark large droplet inoculation (LDI) method.⁵¹ Xu et al. functionalized the surface of MPPM by a three-step process that involved benzophenone grafting, radical polymerization of PDMAEMA, followed by quaternization with alkyl halides.¹⁹ The benzophenone moiety in PEEK polymer was used to self-initiate the grafting of nanometer sized layers of zwitterionic poly(2-methacryloyloxyethyl phosphorylcholine).⁵² Alternatively, vapor-deposited parylene benzophenone coatings were used to covalently bind a rather low loading of chlorhexidine biocide (1.4 ± 0.08 nmol cm⁻²) to prevent *Enterobacter cloacae* biofilm formation.⁵²

In this study, we compare the antimicrobial efficacy of surface attached benzophenone terminated long chain quaternary ammonium salts on a variety of plastic surfaces. The treated surfaces were evaluated using the large droplet test as a new benchmark method used to qualitatively investigate bacterial survival of dry biofilms at the solid–air interface. To that end, our research has focused on the preparation, coating, UV curing, and antimicrobial testing in the dry state of unique surface attached quaternary ammonium biocide chemistries for the permanent antimicrobial modification of plastic, metals, and textile surfaces.⁵³

2. MATERIALS AND METHODS

2.1. Materials. All reagents and solvents were obtained from commercial sources and used as received unless otherwise indicated.

N,N-Dimethyldecylamine was purchased from Alfa, and *N,N*-dimethyloctadecylamine was from Acros. Stock plastic (clear) polyvinyl chloride (CPVC) (cat. 82027-788) and polystyrene (PS) (cat. 89106-754) were supplied by VWR International, polyvinyl chloride (PVC) was sourced from Bow Plastics (cat. 650598), polyether ether ketone (PEEK) was sourced from Drake plastics (cat. KT820NT), high density polyethylene (HDPE) was sourced from ePlastics (cat. HDPENAT0.125SR24X48), and polypropylene (PP) was sourced from Special Coatings USA, LLC. The benzophenone alkyl halides (1a–c, 2a–c, 3a–c; Scheme 1) were prepared as previously described by Saettone.⁴² Synthesis of propyl-dimethyl-(benzoylphenoxy)octadecylammonium bromide 5b was carried out in a Biotage Initiator Microwave Synthesizer (2.45 GHz). The benzophenone-functionalized dansyl quaternary ammonium fluorophore, S1, was obtained as previously described.⁵³ All other experimental details are included in the supplementary section.

2.2. Antimicrobial Compound Characterization. Nuclear magnetic resonance (NMR) experiments were carried out on a 400 MHz Bruker Avance II spectrometer using CDCl₃. ¹H NMR (400 MHz) and ¹³C NMR (100.6 MHz) spectra were referenced to the residual proton and central carbon peak of the solvent. All chemical shifts are given in δ (ppm) relative to the solvent and assigned to atoms on the basis of available 2D spectra for each compound. Thin layer chromatography (TLC) was carried out on silica gel 60 aluminum backed plates, eluting with the solvent system indicated below for each compound. High-resolution mass spectrometry (HRMS) was carried out using electrospray ionization time-of-flight (ESI-ToF) at the Advanced Instrumentation for Molecular Structure (AIMS) laboratory at the University of Toronto. Melting points were measured in open air using a Fisher Scientific melting point apparatus. A Bruker-Nonius Kappa-CCD diffractometer was used to obtain the X-ray information on the crystal structure of 4, which has been deposited with the Cambridge Crystallographic Data Centre and has been assigned the following deposition number: CCDC 1546440.

2.3. Characterization of Antimicrobial Treated Surfaces. Contact angle images of treated and untreated surfaces were taken using a Teli CCD camera equipped with a macro lens and attached perpendicular to the sample surface. Contact angle measurements were performed using SCA20 contact angle software by Data Physics Corporation. X-ray photoelectron spectroscopy (XPS) was performed using a ThermoFisher Scientific K-Alpha, and time-of-flight secondary ion mass spectrometry (ToF-SIMS) was performed using an IonTOF ToF-SIMS IV at the Ontario Centre for the Characterization of Advanced Materials (OCCAM), located at the University of Toronto. Atomic force microscopy (AFM) using an Anasys nanoIR2 equipped with Contact Mode NIR2 Probes (resonance frequency 13 ± 4 kHz, spring constant $0.07\text{--}0.4$ N m⁻¹) and surface profilometry using a KLA-Tencor P16+ surface profilometer were also performed at OCCAM. AFM data were processed using Gwyddion 2.48.⁵⁴ Epifluorescent microscopy was performed using a Leica MZFLIII fluorescence microscope equipped with a PlanApo 1.0 \times objective lens and CFP filter set (excitation filter 436/20 nm, barrier filter 480/40 nm) (Figure S1).

2.4. Antimicrobial Coating Method. Multiple coatings (≤ 3 coats) of 4.4 ± 1 cm² plastic test samples were sprayed using an ESS AD – LG electrospray apparatus (S/N 20073037, Athens, Georgia) set to spray a 1% solution of representative compounds at 150 kPa. Consistent coatings with respect to compound mass and surface coverage (Figure 3) were obtained by spraying samples for 2.5 ± 0.5 s



Figure 2. ORTEP representation of **4** found in the unit cell and selected bond lengths (Å) and bond angles (deg): O(1)–C(3) 1.442(2), O(2)–C(10) 1.221(2), N(1)–C(1) 1.514(2), N(1)–C(19) 1.508(2), C(4)–O(1)–C(3) 119.06 (15), C(19)–N(1)–C(1) 113.21 (14), C(7)–C(10)–C(11) 119.98 (17), C(30)–C(29)–C(28) 113.5 (2).

at an average distance of 45 cm from the spray nozzle. An average of $34.5 \pm 3.3 \mu\text{g cm}^{-2}$ ($n = 3$) of surface coverage was obtained and verified by UV–vis of distilled water-washed samples (Figure S27). Refer to section 2.6 for leaching tests.

2.5. Antimicrobial Curing Method. UV curing of benzophenone-QUAT coated plastics was performed after each coating step using a Novacure spot curing system, set to provide a 300 J UV dose, supplied from a mercury-arc discharge lamp, at a peak intensity of 5000 mW into a reflective curing chamber 2 cm from the light guide source. An intensity of 0.1 W cm^{-2} for 120 s supplied a 12 J cm^{-2} dose per cure, as measured using an EIT UV Power Puck 2.

2.6. Large Droplet Inoculum Antimicrobial Tests. Several bacterial stock cultures were used in these tests. Bacterial test species were grown overnight in 3 g L^{-1} tryptic soy broth at $30 \text{ }^\circ\text{C}$ within a shaking incubator (125 rpm). On the day of testing, 2 mL of growth culture was washed twice by centrifugation at 9000g, replacing the growth media with 4 mL of sterile water (city of Toronto, Canada), diluting cells to $\sim 10^7$ cells/mL. *Arthrobacter* sp. (IAI-3), a Gram-positive bacterium originally isolated from indoor laboratory air, was inoculated onto all treated and control test surfaces.⁵⁵ Lab strains of Gram-negative *Pseudomonas aeruginosa* (PAO1) and Gram-positive *Listeria monocytogenes* (Scott A) were also tested on coated CPVC. These strains were chosen due to their natural resistance to desiccation and to their presence in biofilms found within high-risk environments. The large drop inoculum (LDI) method was used to assess the antimicrobial efficacy of the coating at a solid–air interface. Triplicate coated samples were inoculated with 100 μL bacterial aliquots of subsequently determined concentration using serial dilution followed by spot plating of the inoculum. All samples were placed inside sterile Petri dishes and loosely covered inside a biological safety cabinet to avoid contamination and mimic typical bacterial drying in real world conditions. After drying out of the inoculum on the material surface ($\sim 2\text{--}3 \text{ h}$, 50% RH, room temperature) and after 24 h, samples were placed into separate screw cap 50 mL conical bottom polypropylene tube and vortexed for 60 s in 5 mL of 0.9% physiological saline to rehydrate and dislodge adhered surviving cells. Retrieved cells from each tube were serially diluted 3-fold in 1 mL of 0.9% physiological saline, and 0.1 mL from each dilution ($10^0\text{--}10^3$) was spot-plated onto 3 g/L tryptic soy agar. Plates were then incubated at room temperature for a period of 5–7 d, which allowed for visualization of colony forming units (CFU). At each time point, bacterial survival on the coated samples was compared to survival on triplicate noncoated control surfaces of the same material.

2.7. Antimicrobial Leaching Tests. Qualitative and quantitative tests were performed to determine whether leaching of antimicrobial coating occurred when rinsing samples after curing. Triplicate CPVC control and 2 \times sprayed but non-UV cured pieces were placed onto agar plates streaked with IAI-3 and PAO1 and allowed to incubate at

room temperature for 48 h. This was done to confirm that **5b** does not readily diffuse through tryptic soy agar at biocidal concentrations (Figure S18). Qualitative tests involved the dropwise addition of 40 ppm bromophenol blue dye to the collected rinse solution and observing whether there was a color change from its dianionic purple color to a blue complex formed in the presence of quaternary ammonium cation containing species (LOD = 27.44 nmol). Quantitative testing was performed by rinsing treated, coated but uncured, and control samples and performing UV–vis spectroscopy on collected rinse solutions. Triplicate 4.4 cm^2 clear polyvinyl chloride samples were coated up to three times with **5b** and were vortexed within a 50 mL conical screw-cap tube for 60 s in 5 mL of distilled water. UV–vis spectroscopy was then performed on rinse solutions, and the absorbance was measured at 292 nm, which corresponds to the λ_{max} of **5b**. The following absorbance measurements were then compared against a calibration curve to determine antimicrobial leachate concentration (Figure S27).

2.8. Charge Density Measurement Method.^{15,56} Accessible surface charge density ($\text{N}^+ \text{ cm}^{-2}$) of **5b** coated and UV cured PS was determined on the basis of a fluorescein staining–destaining protocol as previously described. The relation between fluorescein molecules and QAC molecules is 1:1 during this test. Triplicate control and treated samples (4 cm^2) were submerged in 1% (w/v) aqueous fluorescein disodium salt solution and placed on an orbital shaker for 24 h at 150 rpm. Samples were exhaustively rinsed with distilled water to remove unbound fluorescein molecules, as indicated by the visual absence of fluorescein dye within the rinse fluid. Samples were sonicated for 15 min in 9 mL of cetyltrimethylammonium chloride and 1 mL of 0.1 M phosphate buffered saline to liberate bound fluorescein into solution. UV–vis was performed using quartz cuvettes (path length; $L = 1 \text{ cm}$) on collected sonicated solutions, and absorbance was recorded at 501 nm. Concentration (C) and surface charge were calculated using the Beer–Lambert law, with the extinction coefficient value (ϵ_{501}) of $77\,000 \text{ M}^{-1} \text{ cm}^{-1}$.

$$C_{\text{fluorescein}} (\text{mol L}^{-1}) = A_{501} / \epsilon_{501} (\text{M}^{-1} \text{ cm}^{-1}) \times L (\text{cm}) \quad (1)$$

Accessible QAC surface charge density to fluorescein was calculated per centimeter square using the following equation:

$$[\text{N}^+] = \frac{C_{\text{fluorescein}} (\text{mol L}^{-1}) \times V (\text{L}) \times N}{A (\text{cm}^2)} \quad (2)$$

where V represents the volume of collected sonicated solution, N represents Avogadro's number (6.023×10^{23}), and A represents the surface area of a coated sample.

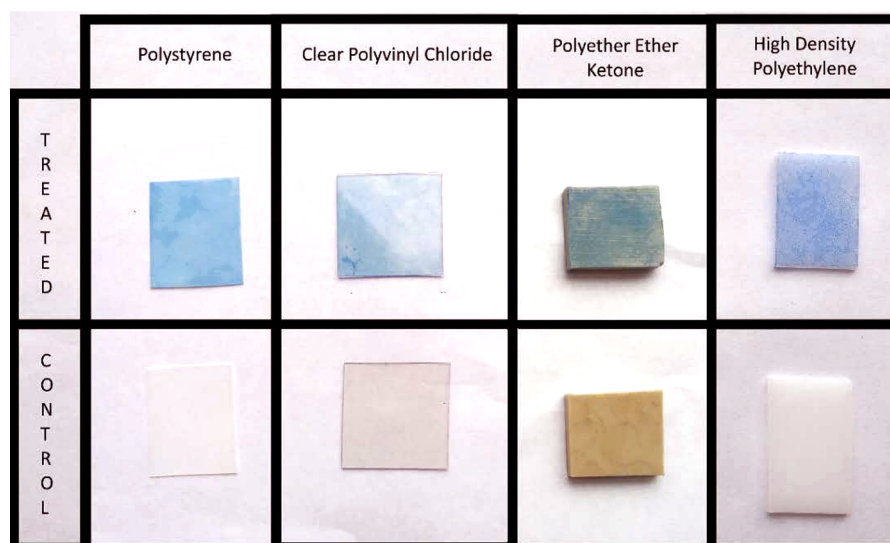


Figure 3. Treated and untreated surfaces stained with bromophenol blue dye.

Table 1. Properties of Surface Attached Benzophenone Antimicrobials

material	adv contact angle ^a (deg)	charge density ^a ([N ⁺] cm ⁻²)	ref
control PS	91.7 ± 1.0	N/A	this work
×1 coating of 5b on PS	63.4 ± 2.5	(6.70 ± 0.60) × 10 ¹⁵	this work
×2 coating of 5b on PS	56.7 ± 1.0	(1.15 ± 0.18) × 10 ¹⁶	this work
×3 coating of 5b on PS	57.8 ± 1.5	(2.00 ± 0.42) × 10 ¹⁶	this work
BPAM-QAC on OTS-glass	69	3.57 × 10 ¹⁵	57

^aAll reported values measured in triplicate.

3. RESULTS AND DISCUSSION

3.1. Synthesis and Characterization of Antimicrobial Quaternary Ammonium Materials. Propyl-dimethyl (benzoylphenoxy)octadecylammonium bromide, **5b**, was previously described by Saettone et al. in 1988 for use as a free radical scavenger in sunscreens.⁴² These authors reacted 4-*O*-(3-*N,N*-dimethylaminopropyl)benzophenone with 1-bromooc-tadecane to obtain compound **5b** in a 50–60% yield. The product was purified by trituration with Et₂O and crystallization from EtOAc and characterized by elemental analysis and melting point.⁴²

In the present research, *N,N*-dimethyldecylamine or *N,N*-dimethyloctadecylamine was quaternized using (*n*-haloalkoxy)-benzophenone in MeCN solution by heating to 100 °C overnight (Scheme 1). This yielded compounds **4**, **5a–c**, **6a–c**, and **7a–c**, as off-white colored powders in good yields. These compounds were further purified by recrystallization from EtOH or EtOH/H₂O mixtures. NMR (¹H and ¹³C) spectroscopy of all compounds, along with HRMS analysis, support their structural identity. Compound **4** was also characterized by single-crystal X-ray diffraction. An ORTEP representation of one of the units of **4** found in the unit cell is displayed in Figure 2. Interestingly, the cationic component of the salt appears folded over on itself, with visible twisting of one of the benzophenone rings to accommodate the presence of the carbonyl oxygen.

The C₁₈ quaternary ammonium salts (**5–7a–c**) are only partially soluble in water, and fully miscible at 1% (w/v) in 70:30 EtOH:H₂O or *i*-PrOH:H₂O solutions. In contrast, the C₁₂ salt (**4**) was found to be fully soluble in H₂O at the same concentration. The relative solubility of these materials in H₂O

or EtOH:H₂O mixtures is in contrast to the closely related alkylated benzophenone quaternary ammonium salts and the hydroxybenzophenone copolymers (Figure 1) prepared by Locklin et al. These materials required formulation in DCM and acetone, respectively, for coating purposes.^{49,57}

3.2. Coating of Benzophenone-Anchored QACs onto Polymeric Surfaces. Compounds **4** and **5b** were selected as the representative C₁₂ and C₁₈ QACs in the evaluation of benzophenone-anchored QAC antimicrobials. The rationale for these choices stems from the relative ease of syntheses, purification, and relatively high solubility of the QAC compounds in aqueous solution. Species **5b** was successfully anchored, in a two-step coating/cure process, to a variety of hard and soft plastic coupons (4 cm² square samples of PS, PVC, PEEK, HDPE, or PP) as well as a plastic fabric (PP). Formulations containing **5b** (1% (w/v) in 70:30 EtOH:H₂O) and optional 0.05% of the dansyl fluorophore **8**, suitable for spray coating onto cleaned substrates using an electrospray apparatus, were prepared and allowed to air-dry. The coated samples were then exposed to broadband UV light at a 5000 mW intensity for 2 min. The coating/UV-curing step was thereafter repeated to ensure coating uniformity.

3.3. Visualization of Antimicrobial Coatings on Test Surfaces. Following application of the compound to the test surface, the presence and uniformity of the coating were confirmed prior to any subsequent antimicrobial efficacy testing. Visualization of the coating was carried out using a water-soluble bromophenol blue stain, which forms an ionic pair with the quaternary ammonium cation present at the surface (Figure 3).

The robustness of the immobilized coating **5b** to withstand routine chemical disinfection and mechanical washing was then

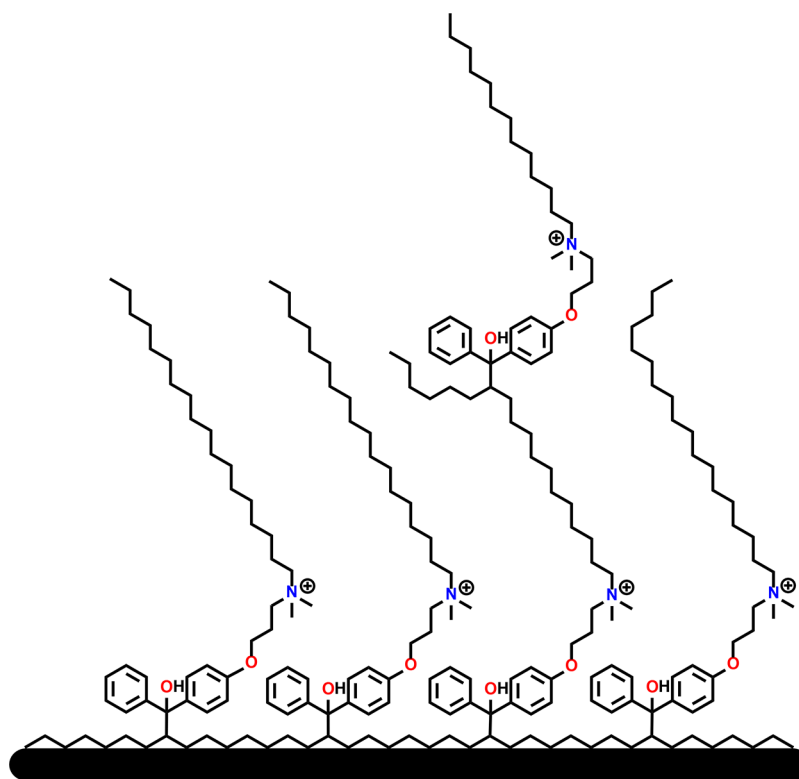


Figure 4. Schematic representation of surface grafted branching of **5b** leading to an increase in coating thickness and charge density on a substrate such as PS.

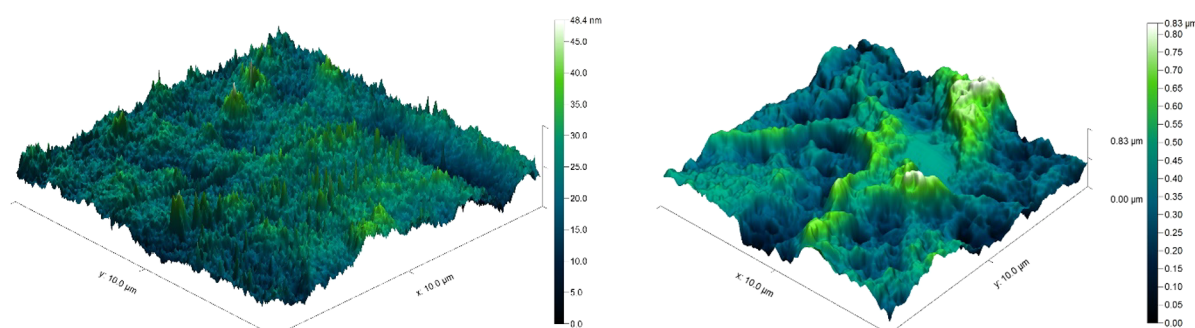


Figure 5. AFM images of PS control (left) and $\times 2$ coating of **5b** on PS (right).

evaluated. Bromophenol blue stained samples were vigorously washed in a detergent solution of cetyltrimethylammonium bromide (CTAB). While the cationic surfactant did remove the staining agent, remaining with bromophenol blue after the CTAB wash confirmed that the coating was still present. For the PP fabric sample, the antimicrobial solution supplemented with a trace ($\sim 0.01\%$ w/v) amount of the dansyl fluorophore S1, prior to electrospaying, was employed to help visualize the antimicrobial coating via epifluorescent microscopy (Figure S1). Successive water rinses failed to remove the fluorophore from the coated surface, indicating that the compound has been successfully immobilized upon UV curing.

3.4. Physical Properties of UV-Cured Thin Films of **5b**.

PS coupons coated with the **5b** antimicrobial, and subsequently UV-cured, exhibited a significant increase in surface hydrophilicity as compared to uncoated controls (Table 1) as expected from adding cationic functional groups to an almost entirely nonpolar polymer surface. Advancing water contact angles of surfaces coated and cured with 1, 2, and 3 coatings

were also compared. These tests show that the initial UV-cured coating had a notable effect on the contact angle, changing from an average of 91.7° for the control polystyrene sample to 63.4° for a single coat. For the subsequent coating layer, the change in contact angle is less dramatic, dropping an additional 8° , and then remains essentially unchanged with the addition of a third layer (Figure 4). Surface charge density measurements of PS samples indicated a high charge value associated with coated materials. Charge density increased as further coating and curing steps are performed corresponding to an increase in the quantity of **5b** applied to the plastic substrate. These values exceeded the charge density values (by 2–4-fold) reported by Locklin et al. Note that the previous (lower) values were found to be sufficient for observing antimicrobial activity in BPAM-QAC materials.⁵⁷

In depth surface characterization and structural analysis of a **5b** coated polystyrene sample was also performed using AFM and SP. To provide surface thickness data, the sample was partially covered using adhesive tape (Scotch 3M) prior to the

coating and curing steps. After treatment, the tape was removed, and the surface was vortexed for 1 min in distilled water to remove any excess coating material and tape residue. This produced a partially treated sample for analysis.

AFM was performed at three locations found along the separation line of the partially coated sample. Coating thickness was determined taking the height differences between the coated and noncoated areas of the sample surface. To limit the impact of coating damage that occurred during tape removal, height measurements were taken at least 15 μm away from the highest point found along the edge of the coated half of the sample.

The average coating thickness of a sample coated with two treatments of **5b** is 366 ± 148 nm, which translates to a height of ~ 80 molecules stacked end-to-end (Figure 5, Table 2). This

Table 2. Thickness Measurements of Surface Attached Benzophenone Antimicrobials

material	ellipsometry (nm)	atomic force microscopy (nm)	surface profilometry (nm)	ref
BPAM-QAC on OTS-glass	42	N/A	N/A	57
$\times 2$ coating of 5b on PS	N/A	366 ± 148	468 ± 159	this work

suggests that multiple layers of coating are applied during each coating and curing step, which presumably immobilizes the antimicrobial to the plastic substrate, as well as extensive grafting of molecules. With regards to data collected by Locklin et al.,⁵⁷ these coating thickness values obtained are ~ 9 times greater, and correlate to an increased charge density value. To confirm accuracy of AFM measurements, SP was also performed on a $500 \mu\text{m}^2$ section along the separation line of the half-treated sample.

Coating structural features were also determined by imaging areas found to be completely within the treated and untreated portions of the samples. These images were obtained at locations $>50 \mu\text{m}$ away from the separation line formed by tape removal. The control sample image indicates a relatively smooth surface with a maximum height variation of ~ 48 nm. The PS treated sample image reveals a significantly rough, random surface. Although these ridges are less structured and generally larger than the antimicrobial nanopili found on the surface of dragonfly wings (~ 200 nm), there are a number of smaller ridges that are similar in size.²⁷ The large variations in ridge height would also correspond to an increased effective surface area when compared to a flat coating and would manifest itself as a higher surface charge density.

To further quantify the coating quality and composition, an XPS analysis (Table 3) was performed on CPVC samples UV-coated with compound **5b**. For comparative analysis of the binding energy peaks relating to the carbon content of the sample (Figures S2–S8), a larger C 1s A (286.6 eV) peak⁵⁸ was

Table 3. Select XPS Survey Data for Control and UV-Coated CPVC Samples of 5b

sample	element	atomic concentration	sensitivity factor
control CPVC	C 1s	81.14	1.00
control CPVC	N 1s	1.00	1.80
CPVC treated with 5b	C 1s	84.24	1.0
CPVC treated with 5b	N 1s	1.46	1.8

detected for the treated sample as compared to the untreated control. This is likely a result of an increase in the quantity of carbon–oxygen bonds found present at the coating survey site. For the XPS peak analysis relating to nitrogen content of the treated and control samples, two peaks relating to N 1s (402.5 eV) and N 1s A (400.0 eV) exhibit large increases (Figure 6) over the control sample.⁵⁹ The larger N 1s A peak corresponds to an increase in carbon–nitrogen bonding, while the N 1s peak corresponds to an increase in cationic nitrogen present within the sample.¹⁹ When comparing elemental analysis data obtained via XPS, there is a 46% increase in atomic concentration at the sample surface. This was seen as a significant increase in nitrogen at the material surface, considering **5b** would consist of 2.27% nitrogen as determined from the empirical formula. Although a pure polystyrene sample would be devoid of nitrogen content, the initial appearance of 1.00 atomic concentration of nitrogen on the control sample was regarded as contamination of the PS sample, either by adsorption of atmospheric nitrogen during its lifespan or by its inclusion during plastic fabrication.

To complement the XPS data collected for surface characterization, time-of-flight secondary ion mass spectrometry (ToF-SIMS) was performed on treated and control CPVC samples (Figure S3).⁶⁰ For this experiment, data collection was performed on a 0.25 mm^2 sample area using bismuth (Bi_3^{2+}) as the primary ion source. Positive and negative ion fragmentation patterns of the treated and control surfaces were analyzed. From the data obtained during ToF-SIMS imaging, fragments peaks relating to benzoylphenolate, tetracarbonyl ammonium, and brominium ions are present on the treated sample. These peaks are consistent with the composition of **5b** and would be expected during negative ion fragmentation, considering the key functional groups used to form benzophenone-anchored QAC antimicrobials. Because bromine is unique to **5b** and absent from the CPVC substrate, it can be used to estimate the total coverage of treated sample, and this was found to be around 84%, as determined using ImageJ measurement software.⁶¹

3.5. Efficacy Testing of Antimicrobial Coating at Solid–Air Interfaces. To ascertain and compare the survival of selected bacterial species when exposed to a QAC-based antimicrobial coating, the large droplet inoculation (LDI) method was performed on treated and control test samples previously prepared using the stated methods. The LDI method was developed and used previously by Wolfaardt et al. for the examination of biofilm-producing microorganisms on solid surfaces,^{55,62} although the origin of this technique has roots in the study of how humidity and desiccation affect the survival of microbes such as *Yersinia pestis*,⁶³ methicillin-resistant *Staphylococcus aureus*,⁶⁴ *Acinetobacter baumannii*,⁶⁵ and other pathogenic microbial strains.⁶⁶ The LDI method (Figure S9) relies on the deposition of a droplet containing a consistent relative quantity of viable cells onto the desired test surface, and allowing the inoculated sample to completely dry within a sterile environment. A standardized 3 h drying period is needed for $100 \mu\text{L}$ of bacterial inoculum at atmospheric humidity and temperature, and this guarantees that all cells have come into contact with the antimicrobial surface. Because the inoculum changes state from liquid to solid during the drying period, this represents the initial contact time for all cells suspended within the inoculum. The desiccated samples are then collected and vortexed for 1 min with an isotonic saline solution to remove any adherent cells, allowing for the optimal recovery of

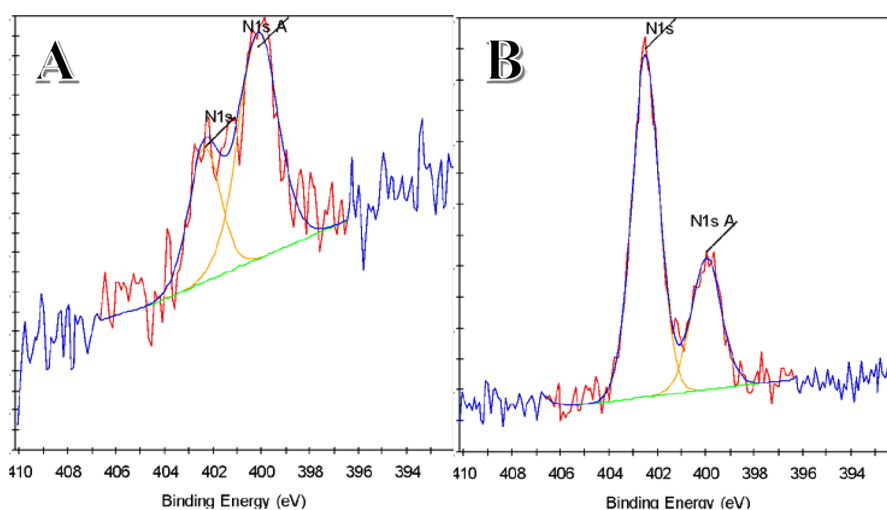


Figure 6. XPS data corresponding to the nitrogen content for the control (A) and **5b** coated (B) PS samples.

previously inoculated cells.⁵⁵ The resulting collection fluid is then serially diluted and plated on an appropriate growth media and incubated accordingly, allowing for the enumeration of viable colony forming units.

The LDI method was developed to simulate real-world conditions that result in the deposition of concentrated bacteria onto available material surfaces, while also providing a consistent and reproducible approach across multiple sample materials.⁵⁵ This method best represents the deposition of aerosol- and droplet-suspended microbial organisms, which have long been considered a primary method for pathogenic transmission. This, in turn, has influenced aerosol reduction methods,⁶⁷ standard biology practices and procedures, and healthcare and institutional design choices.^{4,67} This is in comparison to ISO 22196/JIS Z 2801 and ASTM E2149, which are commonly used standard procedures when assessing antimicrobial activity on material surfaces.⁶⁸ The ISO 22196:2011 and the closely related JIS Z 2801:2010 methods rely on covering the inoculated microbial samples with a coverslip. This coverslip keeps the inoculated surface consistently wet and is less likely to simulate one where a microbe-containing droplet has landed and dried out. As compared to the LDI method, ISO 22196/JIS Z 2801 suspends a dilute inoculum over a large surface area at high humidity instead of forcing cells directly into contact with the antimicrobial coating by evaporation of the inoculation liquid. Cell death due to dehydration is addressed in the LDI method by using desiccation-resistant species as model organisms. The ASTM E2149 procedure operates by dynamically shaking samples within an inoculated buffered solution. This method also relies on solid–liquid-mediated interactions between material and microbes, but can lead to biased results from material leachates, biofilm growth on and within test materials, and does not force cells directly into contact with the material surface.⁶⁸

To increase the consistency and reduce environmental variability between test samples, factors such as growth phase and nutrient availability were carefully established. To control for growth factors and lifecycle, broth cultures were grown to the late exponential phase, occurring 16–18 h after broth inoculation.⁵⁵ For nutrient control, the cultured cells were washed twice with sterilized tap water to remove nutrients, and to limit experiment-imposed osmotic shock while desiccating.

The LDI method also provides a more consistent measure of bacterial inoculation when compared to spray inoculation tests, as spray-based techniques rely on random droplet placement onto coated, control, and other areas not accounted for during analysis within the spray chamber.^{15,68} Additional benefits of using a large droplet over an aerosol spray include the known application of a greater number of cells to a sample surface,^{15,68,69} increased cell viability during desiccation,⁵⁵ and a reduced potential for accidental exposure to pathogenic-containing aerosols during testing.

For these tests, three bacterial strains were used for the evaluation of test samples. The first was an airborne bacterial isolate of *Arthrobacter* species (IAI-3) used to provide a model organism for microbiological testing when comparing bacterial survival on treated and control samples. The *Arthrobacter* genus represents a Gram-positive, weakly motile, nonsporulating bacteria commonly found in soil. This strain was isolated by Wolfaardt et al. for the purpose of studying nonaqueous biofilms and interspecies interactions during biofilm formation, and is notable for its ability to resist desiccation at room temperature.^{55,69} With the additional demonstrated inability to form spores, and preferred growth temperature of 20–30 °C, results obtained using IAI-3 are highly representative of general solid–air interactions because these factors prevent any impact on viability of these cells during testing. *P. aeruginosa* (PAO1) was another bacterial species used to determine whether QAC-coated plastic surfaces could effectively kill Gram-negative bacteria. This species is of medical importance and has been studied extensively for its ability to produce biofilms, cause secondary hospital infections, and resist antimicrobial agents.^{1,4} *Listeria monocytogenes* (Scott A), a Gram-positive bacterial species capable of surviving in the absence or presence of oxygen and an important food borne pathogen, was also investigated. This bacterial strain is a clinical isolate retrieved during a 1983 listeriosis outbreak in Massachusetts, and has been well characterized and widely used for testing in food and healthcare related industries.⁷⁰

The Gram-positive indoor air isolate *Arthrobacter* sp. (IAI-3) was used as a representative member of the indoor bacterial flora, members of which continuously undergo deposition from the air onto exposed surfaces. While these species may not be dangerous to healthy individuals, they can lead to infection in patients with a compromised immune system, and are also able

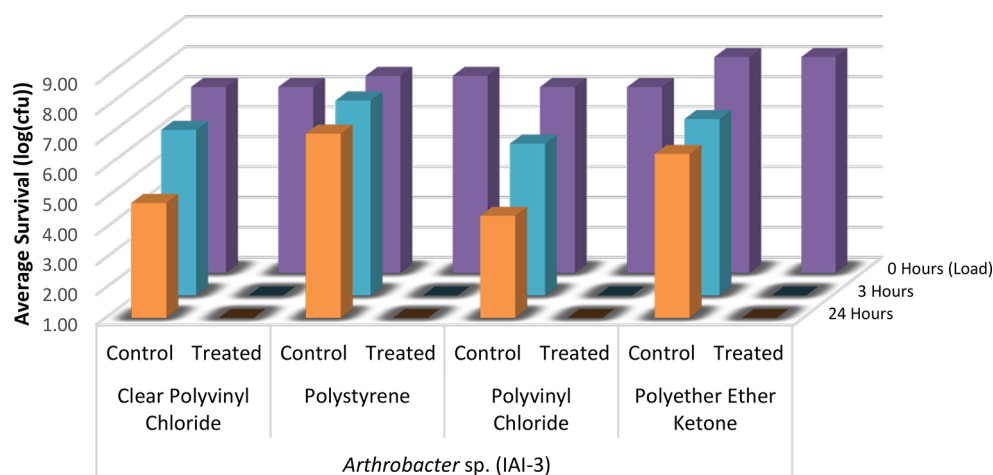


Figure 7. Graph depicting the average survivability of *Arthrobacter sp.* when inoculated onto a variety of **5b** treated and control sample materials. The measurement at 0 h (log 7 CFU) indicated the initial number of bacterial cells being inoculated onto the surface material and was determined concurrently to inoculation.

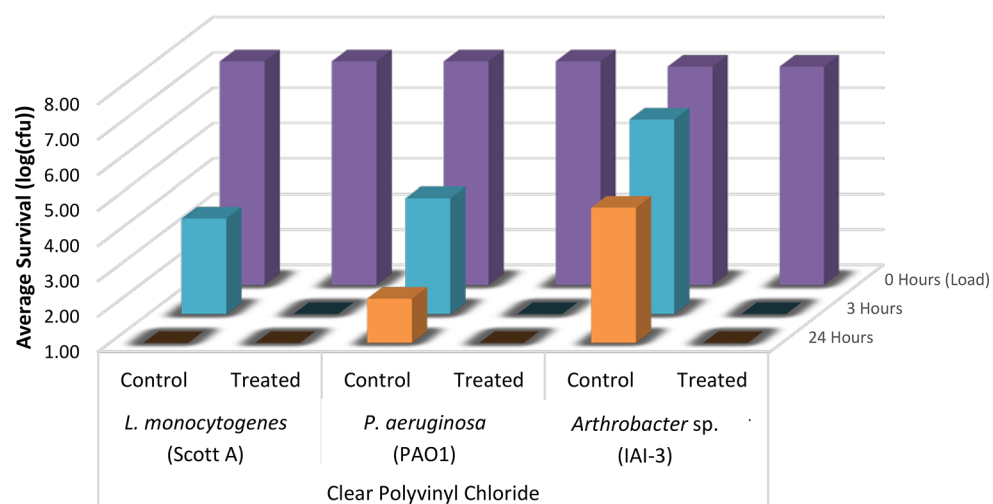


Figure 8. Graph depicting the average survival of *L. monocytogenes*, *P. aeruginosa*, and *Arthrobacter sp.*, when inoculated onto QAC-treated (**5b**) and control samples of CPVC.

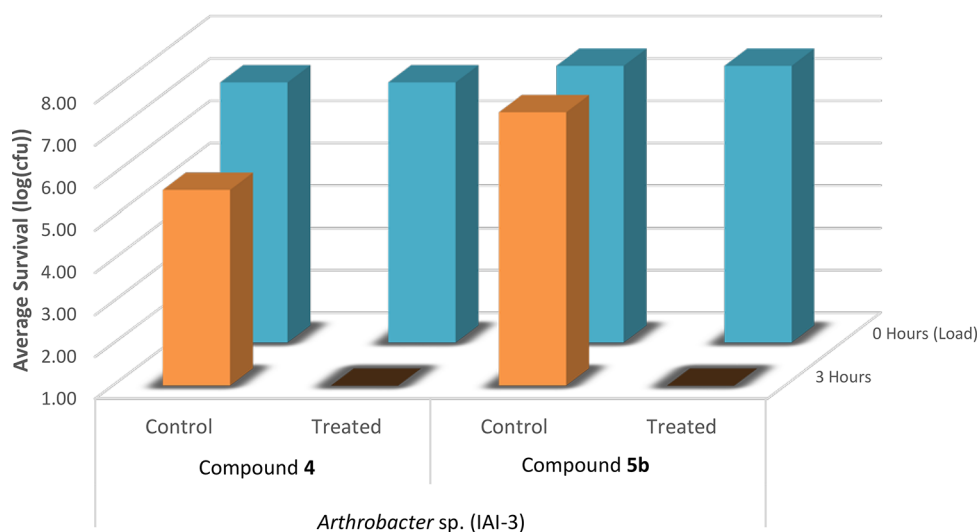


Figure 9. Graph depicting the average survival of *Arthrobacter sp.* when inoculated onto a variety of **4** and **5b** treated and control samples.

to protectively provide niches in which exogenous pathogens in the hospital environment survive.⁵⁵ *Arthrobacter* sp. survival was tested on several clinically relevant plastics, and, in each case, no surviving cells were detected on the coated surfaces, while the uncoated control surfaces still contained high cell counts (log 4–6 CFU) even 24 h after inoculation and drying (Figure 7). Antimicrobial efficacy on treated PEEK plastic is of particular interest, because it is often used in medical implants due to its high resistance to chemical and physical stress.

The coating was also tested against two bacteria strains, which are often implicated in HCAI infections. The Gram-negative *P. aeruginosa* and Gram-positive *L. monocytogenes* were unable to survive after 3 h when inoculated onto coated CPVC surfaces (Figure 8). The effectiveness of the compound against both Gram-positive and Gram-negative bacterial species suggests that the treated surfaces are nonselective.

When subjected to the same antimicrobial testing methods mentioned above, compound 4 exhibited antimicrobial properties similar to those of materials coated with compound 5b (Figure 9).

4. CONCLUSION

Microbiological testing with the LDI protocol showed that benzophenone-based QAC antimicrobial coatings are effective in preventing the survival of both Gram-positive and Gram-negative bacterial strains at solid–air interfaces. These tests, along with bromophenol blue staining, show that these antimicrobial compounds can be applied across a wide selection of available plastic materials. This result is particularly exciting because these coatings can be applied to plastics used in clinical settings, food-processing plants, and many other high-risk environments to prevent the transfer of pathogenic microorganisms across solid surfaces, and to prevent biofilm development.

■ ASSOCIATED CONTENT

Supporting Information

The Supporting Information is available free of charge on the ACS Publications website at DOI: 10.1021/acsami.7b07363.

Detailed preparation and characterization for all compounds and coatings provided including NMR (¹H, ¹³C, and 2D experiments), contact angle, XPS and ToF-SIMS, AFM, and SP data (PDF)

■ AUTHOR INFORMATION

Corresponding Author

*Tel.: (416) 979-5000, ext 2260. E-mail: daniel.foucher@ryerson.ca.

ORCID

Daniel A. Foucher: 0000-0002-5918-5391

Notes

The authors declare no competing financial interest.

■ ACKNOWLEDGMENTS

This publication was supported in part by NSERC Engage, by Whoosh! Inc., and by Nanosafe Technologies. We would like to thank Rana Sodhi and Peter Brodersen from the University of Toronto OCCAM Surface Analysis Centre for the acquisition and interpretation of XPS, ToF-SIMS, AFM, and surface profilometry data. We also thank Drs. Joseph McPhee, Robert

A. Gossage, Marthinus Kroukamp, and W. Curtis White for very helpful comments and suggestions.

■ REFERENCES

- (1) Page, K.; Wilson, M.; Parkin, I. P. Antimicrobial Surfaces and Their Potential in Reducing the Role of the Inanimate Environment in the Incidence of Hospital-Acquired Infections. *J. Mater. Chem.* **2009**, *19*, 3819–3831.
- (2) World Health Organization. *Antimicrobial Resistance: Global Report on Surveillance*; 2014.
- (3) Bryers, J. D. Medical Biofilms. *Biotechnol. Bioeng.* **2008**, *100*, 1–18.
- (4) Hota, S.; Hirji, Z.; Stockton, K.; Lemieux, C.; Dedier, H.; Wolfaardt, G.; Gardam, M. A. Outbreak of Multidrug-Resistant *Pseudomonas Aeruginosa* Colonization and Infection Secondary to Imperfect Intensive Care Unit Room Design. *Infect. Control Hosp. Epidemiol.* **2009**, *30*, 25–33.
- (5) Carey, D. E.; McNamara, P. J. The Impact of Triclosan on the Spread of Antibiotic Resistance in the Environment. *Front. Microbiol.* **2015**, *6*, 1–11.
- (6) Percival, S. L.; Suleman, L.; Donelli, G. Healthcare-Associated Infections, Medical Devices and Biofilms: Risk, Tolerance and Control. *J. Med. Microbiol.* **2015**, *64*, 323–334.
- (7) Isquith, A. J.; Abbott, E. A.; Walters, P. A. Surface-Bonded Antimicrobial Activity of an Organosilicon Quaternary Ammonium Chloride. *Appl. Microbiol.* **1972**, *24*, 859–863.
- (8) Higgs, B. S.; White, W. C. Solid Antimicrobial. U.S. Patent 590649613, 1991.
- (9) Cavallaro, A.; Mierczynska, A.; Barton, M.; Majewski, P.; Vasilev, K. Influence of Immobilized Quaternary Ammonium Group Surface Density on Antimicrobial Efficacy and Cytotoxicity. *Biofouling* **2016**, *32*, 13–24.
- (10) Asri, L. A. T. W.; Crismaru, M.; Roest, S.; Chen, Y.; Ivashenko, O.; Rudolf, P.; Tiller, J. C.; Van Der Mei, H. C.; Loontjens, T. J. A.; Busscher, H. J. A Shape-Adaptive, Antibacterial-Coating of Immobilized Quaternary-Ammonium Compounds Tethered on Hyperbranched Polyurea and Its Mechanism of Action. *Adv. Funct. Mater.* **2014**, *24*, 346–355.
- (11) Jońca, J.; Tukaj, C.; Werel, W.; Mizerska, U.; Fortuniak, W.; Chojnowski, J. Bacterial Membranes Are the Target for Antimicrobial Polysiloxane-Methacrylate Copolymer. *J. Mater. Sci.: Mater. Med.* **2016**, *27*, 1–14.
- (12) Milović, N. M.; Wang, J.; Lewis, K.; Klivanov, A. M. Immobilized N-Alkylated Polyethylenimine Avidly Kills Bacteria by Rupturing Cell Membranes with No Resistance Developed. *Biotechnol. Bioeng.* **2005**, *90*, 715–722.
- (13) Li, P.; Poon, Y. F.; Li, W.; Zhu, H.-Y.; Yeap, S. H.; Cao, Y.; Qi, X.; Zhou, C.; Lamrani, M.; Beuerman, R. W.; Kang, E.-T.; Mu, Y.; Li, C. M.; Chang, M. W.; Jan Leong, S.; Chan-Park, M. B. A Polycationic Antimicrobial and Biocompatible Hydrogel with Micro Membrane Suctioning Ability. *Nat. Mater.* **2011**, *10*, 149–156.
- (14) Zou, P.; Laird, D.; Riga, E. K.; Deng, Z.; Dorner, F.; Perez-Hernandez, H.-R.; Guevara-Solarte, D. L.; Steinberg, T.; Al-Ahmad, A.; Lienkamp, K. Antimicrobial and Cell- Compatible Surface-Attached Polymer Networks – How the Correlation of Chemical Structure to Physical and Biological Data Leads to a Modified Mechanism of Action. *J. Mater. Chem. B* **2015**, *3*, 6224–6238.
- (15) Tiller, J. C.; Liao, C. J.; Lewis, K.; Klivanov, A. M. Designing Surfaces That Kill Bacteria on Contact. *Proc. Natl. Acad. Sci. U. S. A.* **2001**, *98*, 5981–5985.
- (16) Tiller, J. C.; Lee, S. B.; Lewis, K.; Klivanov, A. M. Polymer Surfaces Derivatized with Poly(vinyl-N-Hexylpyridinium) Kill Airborne and Waterborne Bacteria. *Biotechnol. Bioeng.* **2002**, *79*, 465–471.
- (17) Lewis, K.; Klivanov, A. M. Surpassing Nature: Rational Design of Sterile-Surface Materials. *Trends Biotechnol.* **2005**, *23*, 343–348.
- (18) ASTM E2149-13a Standard Test Method for Determining the Antimicrobial Activity of Antimicrobial Agents Under Dynamic Contact Conditions, 2013.

- (19) Yang, Y.-F.; Hu, H.-Q.; Li, Y.; Wan, L.-S.; Xu, Z.-K. Membrane Surface with Antibacterial Property by Grafting Polycation. *J. Membr. Sci.* **2011**, *376*, 132–141.
- (20) Huang, J.; Murata, H.; Koepsel, R. R.; Russell, A. J.; Matyjaszewski, K. Antibacterial Polypropylene via Surface-Initiated Atom Transfer Radical Polymerization. *Biomacromolecules* **2007**, *8*, 1396–1399.
- (21) Ferreira, L.; Zumbuehl, A. Non-Leaching Surfaces Capable of Killing Microorganisms on Contact. *J. Mater. Chem.* **2009**, *19*, 7796–7806.
- (22) Bieser, A. M.; Tiller, J. C. Mechanistic Considerations on Contact-Active Antimicrobial Surfaces with Controlled Functional Group Densities. *Macromol. Biosci.* **2011**, *11*, 526–534.
- (23) Siedenbiedel, F.; Tiller, J. C. Antimicrobial Polymers in Solution and on Surfaces: Overview and Functional Principles. *Polymers* **2012**, *4*, 46–71.
- (24) Yatvin, J.; Gao, J.; Locklin, J. Durable Defense: Robust and Varied Attachment of Non-Leaching Poly⁺-Onium⁺ bactericidal Coatings to Reactive and Inert Surfaces. *Chem. Commun.* **2014**, *50*, 9433–9442.
- (25) Kugler, R.; Bouloussa, O.; Rondelez, F. Evidence of a Charge-Density Threshold for Optimum Efficiency of Biocidal Cationic Surfaces. *Microbiology* **2005**, *151*, 1341–1348.
- (26) Murata, H.; Koepsel, R. R.; Matyjaszewski, K.; Russell, A. J. Permanent, Non-Leaching Antibacterial surfaces—2: How High Density Cationic Surfaces Kill Bacterial Cells. *Biomaterials* **2007**, *28*, 4870–4879.
- (27) Bandara, C. D.; Singh, S.; Afara, I. O.; Tesfamichael, T.; Wolff, A.; Ostrikov, K.; Oloyede, A. Bactericidal Effects of Natural Nanotopography of Dragonfly Wing on Escherichia Coli. *ACS Appl. Mater. Interfaces* **2017**, *9*, 6746.
- (28) Appendini, P.; Hotchkiss, J. H. Review of Antimicrobial Food Packaging. *Innovative Food Sci. Emerging Technol.* **2002**, *3*, 113–126.
- (29) Gottenbos, B.; Van Der Mei, H. C.; Klatter, F.; Nieuwenhuis, P.; Busscher, H. J. In Vitro and in Vivo Antimicrobial Activity of Covalently Coupled Quaternary Ammonium Silane Coatings on Silicone Rubber. *Biomaterials* **2002**, *23*, 1417–1423.
- (30) Körner, M.; Prucker, O.; Rühle, J. Kinetics of the Generation of Surface-Attached Polymer Networks through C, H-Insertion Reactions. *Macromolecules* **2016**, *49*, 2438–2447.
- (31) Ma, H.; Davis, R. H.; Bowman, C. N. A Novel Sequential Photoinduced Living Graft Polymerization. *Macromolecules* **2000**, *33*, 331–335.
- (32) Rohr, T.; Ogletree, D. F.; Svec, F.; Fréchet, J. M. J. Surface Functionalization of Thermoplastic Polymers for the Fabrication of Microfluidic Devices by Photoinitiated Grafting. *Adv. Funct. Mater.* **2003**, *13*, 264–270.
- (33) Carbone, N. D.; Ene, M.; Lancaster, J. R.; Koberstein, J. T. Kinetics and Mechanisms of Radical-Based Branching/cross-Linking Reactions in Preformed Polymers Induced by Benzophenone and Bis-Benzophenone Photoinitiators. *Macromolecules* **2013**, *46*, 5434–5444.
- (34) Prucker, O.; Naumann, C. A.; Rühle, J.; Knoll, W.; Frank, C. W. Photochemical Attachment of Polymer Films to Solid Surfaces via Monolayers of Benzophenone Derivatives. *J. Am. Chem. Soc.* **1999**, *121*, 8766–8770.
- (35) Jayaprakash, J. D.; Samuel, S.; Ruhe, J. A Facile Photochemical Surface Modification Technique for the Generation of Microstructured Fluorinated Surfaces. *Langmuir* **2004**, *20*, 10080–10085.
- (36) Chang, B. J.; Prucker, O.; Groh, E.; Wallrath, A.; Dahm, M.; Rühle, J. Surface-Attached Polymer Monolayers for the Control of Endothelial Cell Adhesion. *Colloids Surf., A* **2002**, *198–200*, 519–526.
- (37) Naumann, C. A.; Prucker, O.; Lehmann, T.; Rühle, J.; Knoll, W.; Frank, C. W. The Polymer-Supported Phospholipid Bilayer: Tethering as a New Approach to Substrate-Membrane Stabilization. *Biomacromolecules* **2002**, *3*, 27–35.
- (38) Leshem, B.; Sarfati, G.; Novoa, A.; Breslav, I.; Marks, R. S. Photochemical Attachment of Biomolecules onto Fibre-Optics for Construction of a Chemiluminescent Immunosensor. *Luminescence* **2004**, *19*, 69–77.
- (39) Hartleb, W.; Saar, J. S.; Zou, P.; Lienkamp, K. Just Antimicrobial Is Not Enough: Toward Bifunctional Polymer Surfaces with Dual Antimicrobial and Protein-Repellent Functionality. *Macromol. Chem. Phys.* **2016**, *217*, 225–231.
- (40) Pahnke, J.; Rühle, J. Attachment of Polymer Films to Aluminium Surfaces by Photochemically Active Monolayers of Phosphonic Acids. *Macromol. Rapid Commun.* **2004**, *25*, 1396–1401.
- (41) Griep-Raming, N.; Karger, M.; Menzel, H. Using Benzophenone-Functionalized Phosphonic Acid To Attach Thin Polymer Films to Titanium Surfaces. *Langmuir* **2004**, *20*, 11811–11814.
- (42) Saettoni, M. F.; Alderigi, C.; Giannaccini, B.; Anselmi, C.; Rossetti, M. G.; Scotton, M.; Cerini, R. Substantivity of Sunscreens-Preparation and Evaluation of Some Quaternary Ammonium Benzophenone Derivatives. *Int. J. Cosmet. Sci.* **1988**, *10*, 99–109.
- (43) Dormán, G.; Prestwich, G. D. Benzophenone Photophores in Biochemistry. *Biochemistry* **1994**, *33*, 5661–5673.
- (44) Swan, D. G.; Amos, R. A.; Everson, T. P. Photoactivatable Cross-Linking Agents Containing Charged Groups for Water Solubility. U.S. Patent US6077698, 2000.
- (45) Prestwich, G.; Dormán, G.; Elliott, J.; Marecak, D.; Chaudhary, A. Benzophenone Photoprobes for Phosphoinositides, Peptides and Drugs. *Photochem. Photobiol.* **1997**, *65*, 222–234.
- (46) Green, P. N.; Green, W. A. Benzophenone Derivatives. Patent EP0279475A2, 1990.
- (47) Ruckert, D.; Geuskens, G. Surface Modification of polymers—IV. Grafting of Acrylamide via an Unexpected Mechanism Using a Water Soluble Photo-Initiator. *Eur. Polym. J.* **1996**, *32*, 201–208.
- (48) Barbey, R.; Lavanant, L.; Paripovic, D.; Schüwer, N.; Sugnaux, C.; Tugulu, S.; Klok, H. -Polymer Brushes via Surface-Initiated Controlled Radical Polymerization: Synthesis, Characterization, Properties, and Applications. *Chem. Rev.* **2009**, *109*, 5437–5527.
- (49) Dhende, V. P.; Samanta, S.; Jones, D. M.; Hardin, I. R.; Locklin, J. One-Step Photochemical Synthesis of Permanent, Nonleaching, Ultrathin Antimicrobial Coatings for Textiles and Plastics. *ACS Appl. Mater. Interfaces* **2011**, *3*, 2830–2837.
- (50) Locklin, J. Photochemical Cross-Linkable Polymers, Methods of Making Photochemical Cross-Linkable Polymers, and Methods of Making Articles Containing Photochemical Cross-Linkable Polymers. US Patent 2014024286 A1, 2014.
- (51) Porosa, L.; Mocella, A.; Wolfaardt, G.; Foucher, D. UV-Cured Benzophenone Terminated Quaternary Ammonium Antimicrobials for Surfaces. WO Patent 2014089680 A1, 2011.
- (52) Chang, C.-H.; Yeh, S.-Y.; Lee, B.-H.; Hsu, C.-W.; Chen, Y.-C.; Chen, C.-J.; Lin, T.-J.; Hung-Chih Chen, M.; Huang, C.-T.; Chen, H.-Y. Compatibility Balanced Antibacterial Modification Based on Vapor-Deposited Parylene Coatings for Biomaterials. *J. Mater. Chem. B* **2014**, *2*, 8496–8503.
- (53) Porosa, L. M.; Mistry, K. B.; Mocella, A.; Deng, H.; Hamzehi, S.; Caschera, A.; Lough, A. J.; Wolfaardt, G.; Foucher, D. a. Synthesis, Structures and Properties of Self-Assembling Quaternary Ammonium Dansyl Fluorescent Tags for Porous and Non-Porous Surfaces. *J. Mater. Chem. B* **2014**, *2*, 1509.
- (54) Nečas, D.; Klapetek, P. Gwyddion: An Open-Source Software for SPM Data Analysis. *Open Phys.* **2012**, *10*, 181–189.
- (55) Ronan, E.; Yeung, C. W.; Hausner, M.; Wolfaardt, G. M. Interspecies Interaction Extends Bacterial Survival at Solid-Air Interfaces. *Biofouling* **2013**, *29*, 1087–1096.
- (56) van de Lagemaat, M.; Grotenhuis, A.; van de Belt-Gritter, B.; Roest, S.; Loontjens, T. J. A.; Busscher, H. J.; van der Mei, H. C.; Ren, Y. Comparison of Methods to Evaluate Bacterial Contact-Killing Materials. *Acta Biomater.* **2017**, *59*, 139.
- (57) Gao, J.; Huddleston, N. E.; White, E. M.; Pant, J.; Handa, H.; Locklin, J. Surface Grafted Antimicrobial Polymer Networks with High Abrasion Resistance. *ACS Biomater. Sci. Eng.* **2016**, *2*, 1169–1179.
- (58) Shchukarev, A.; Korolkov, D. XPS Study of Group IA Carbonates. *Open Chem.* **2004**, *2*, 347–362.
- (59) Rignanese, G.; Pasquarello, A.; Charlier, J.; Gonze, X.; Car, R. Nitrogen Incorporation at Si(001)-SiO₂ Interfaces: Relation between

N 1s Core-Level Shifts and Microscopic Structure. *Phys. Rev. Lett.* **1997**, *79*, 5174–5177.

(60) Goacher, R. E.; Drajeremic, G.; Master, E. R. Expanding the Library of Secondary Ions That Distinguish Lignin and Polysaccharides in Time-of-Flight Secondary Ion Mass Spectrometry Analysis of Wood. *Anal. Chem.* **2011**, *83*, 804–812.

(61) Abràmoff, M. D.; Magalhães, P. J.; Ram, S. J. Image Processing with imageJ. *Biophotonics Int.* **2004**, *11*, 36–41.

(62) Stone, W.; Kroukamp, O.; McKelvie, J.; Korber, D. R.; Wolfaardt, G. M. Microbial Metabolism in Bentonite Clay: Saturation, Desiccation and Relative Humidity. *Appl. Clay Sci.* **2016**, *129*, 54–64.

(63) Rose, L. J.; Donlan, R.; Banerjee, S. N.; Arduino, M. J. Survival of *Yersinia Pestis* on Environmental Surfaces. *Appl. Environ. Microbiol.* **2003**, *69*, 2166–2171.

(64) Makison, C.; Swan, J. The Effect of Humidity on the Survival of MRSA on Hard Surfaces. *Indoor Built Environ.* **2006**, *15*, 85–91.

(65) Wendt, C.; Dietze, B.; Dietz, E.; Rüden, H. Survival of *Acinetobacter Baumannii* on Dry Surfaces. *J. Clin. Microbiol.* **1997**, *35*, 1394–1397.

(66) Yazgi, H.; Uyanik, M. H.; Ertek, M.; Aktas, A. E.; İgan, H.; Ayyildiz, A. Survival of Certain Nosocomial Infectious Agents on the Surfaces of Various Covering Materials. *Turk J. Med. Sci.* **2009**, *39*, 619–622.

(67) Ijaz, M. K.; Zargar, B.; Wright, K. E.; Rubino, J. R.; Sattar, S. A. Generic Aspects of the Airborne Spread of Human Pathogens Indoors and Emerging Air Decontamination Technologies. *Am. J. Infect. Control* **2016**, *44*, S109–S120.

(68) Green, J.-B. D.; Fulghum, T.; Nordhaus, M. A. A Review of Immobilized Antimicrobial Agents and Methods for Testing. *Biointerphases* **2011**, *6*, MR13–MR28.

(69) Stone, W.; Kroukamp, O.; Korber, D. R.; McKelvie, J.; Wolfaardt, G. M. Microbes at Surface-Air Interfaces: The Metabolic Harnessing of Relative Humidity, Surface Hygroscopicity, and Oligotrophy for Resilience. *Front. Microbiol.* **2016**, *7*, 1–15.

(70) Briers, Y.; Klumpp, J.; Schuppler, M.; Loessner, M. J. Genome Sequence of *Listeria Monocytogenes* Scott A, a Clinical Isolate from a Food-Borne Listeriosis Outbreak. *J. Bacteriol.* **2011**, *193*, 4284–4285.